Self-consistent electric field-induced dipole interaction of colloidal spheres, cubes, rods, and dumbbells

Bas W. Kwaadgras, René van Roij, and Marjolein Dijkstra

Citation: The Journal of Chemical Physics **140**, 154901 (2014); doi: 10.1063/1.4870251
View online: http://dx.doi.org/10.1063/1.4870251
View Table of Contents: http://scitation.aip.org/content/aip/journal/jcp/140/15?ver=pdfcov
Published by the AIP Publishing

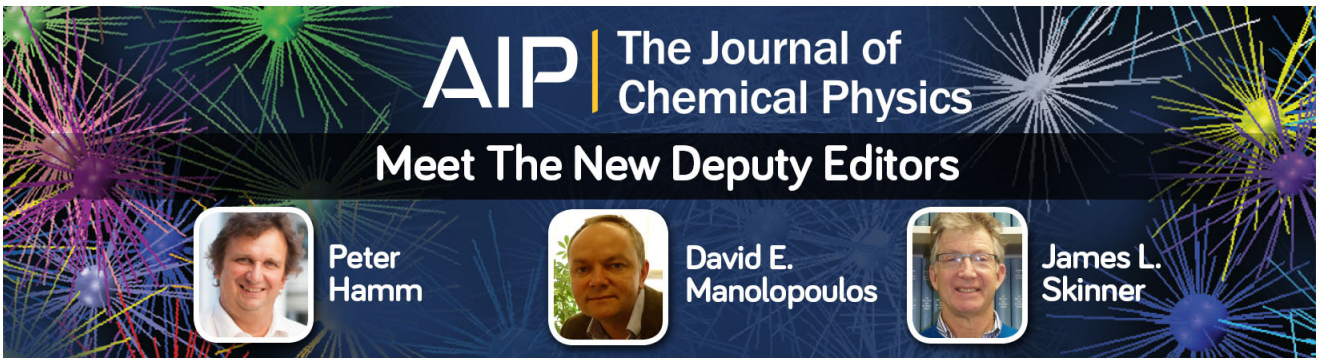

Self-consistent electric field-induced dipole interaction of colloidal spheres, cubes, rods, and dumbbells

Bas W. Kwaadgras,[1] René van Roij,[2] and Marjolein Dijkstra[1]
[1]*Debye Institute for Nanomaterials Science, Utrecht University, Princetonplein 5, 3584 CC Utrecht, The Netherlands*
[2]*Institute for Theoretical Physics, Utrecht University, Leuvenlaan 4, 3584 CE Utrecht, The Netherlands*

(Received 10 November 2013; accepted 21 March 2014; published online 15 April 2014)

When calculating the interaction between electric field-induced dipoles, the dipole moments are often taken to be equal to their polarizability multiplied by the external electric field. However, this approach is not exact, since it does not take into account the fact that particles with a dipole moment affect the local electric field experienced by other particles. In this work, we employ the Coupled Dipole Method to calculate the electric-field-induced dipole pair interaction self-consistently: that is, we take into account many-body effects on the individual induced dipole moments. We calculate interactions of particles with nonvanishing dimensions by splitting them up into self-consistently inducible "chunks" of polarizable matter. For point dipoles, spheres, cubes, rods, and dumbbells, we discuss the differences and commonalities between our self-consistent approach and the aforementioned approach of pre-assigning dipole moments to either the point dipoles or, in the case of spatially extended particles, to the chunks making up the particle. © *2014 AIP Publishing LLC*. [http://dx.doi.org/10.1063/1.4870251]

I. INTRODUCTION

Electric field-induced self-assembly of colloidal particles is an area with tremendous potential for technical applications. Unsurprisingly, therefore, experimental studies in which electric fields are used to orientationally and/or positionally organize particles are commonplace today,[1–7] as are simulation studies in this area.[8–12] The simultaneous progress in particle synthesis[13,14] continues to increase the diversity of systems suitable for electric-field induced assembly. Nowadays, particles of many sizes, materials, and anisotropic shapes can be synthesized and the problem of theoretically describing the interaction of these anisotropic particles with the electric field and with each other under the influence of the electric field becomes less and less trivial. In fact, as we will show in this work, even the dipolar interaction between a pair of spherical particles is nontrivial.

We can roughly distinguish two processes by which an electric field can induce organization in a system of colloids that possess no permanent dipole, namely individual alignment and interparticle interactions. Individual alignment occurs if a particle has an anisotropic polarizability causing a potential-energy minimum at orientation(s) where the induced dipole moment is strongest. Interparticle interactions are the result of interactions between the induced dipole moments of two or more particles and are often crucial for electric field-induced formation of spatially ordered structures. These interparticle interactions are the focus of this paper.

Theoretically, these interactions have often been described by assigning a permanent dipole moment, equal to the particle polarizability multiplied by the applied electric field, to each particle and then making use of the well-known expression for the interaction energy between two electric point dipoles.[15] This approach, which we will refer to as the "single permanent dipoles" (SPD) approach, is nonexact for two reasons. The first is that a particle has a finite size and its polarization will therefore be spread out over its volume instead of concentrated in a point. This problem can be overcome by splitting up the particle into a sufficiently large number of "chunks" of matter, assigning to each chunk a (smaller) polarization, and then summing the interactions between all chunk pairs.[16] We dub this approach the "cluster of permanent dipoles" (CPD) approach. The second nonexactness arises because we neglected the influence that the particles have on each other's induced dipole moment. Since each particle that gains a dipole moment produces an electric field, it will affect the local electric field experienced by all other particles, which is therefore no longer equal to the external (applied) electric field. Calculating each particle's (or particle chunk's) dipole moment turns out to be a system of linear equations that can be solved self-consistently within the framework of the Coupled Dipole Method (CDM).[17–20]

The CDM was proposed by Renne and Nijboer in the 1960s to self-consistently calculate the eigenmodes of a system of atoms with inducible dipole moments (Lorentz atoms) using large-matrix manipulation and, by summing the frequencies of these eigenmodes, to calculate the van der Waals (VdW) interaction energy between clusters of atoms.[17,18,21–24] Discrete dipoles have also been used for scattering calculations within the Discrete Dipole Approximation, which involves an incident oscillating electric field.[25–28] By considering a permanent electric field instead, the polarizability of particles of various shapes has been investigated as well,[19,20,29] resulting, where comparison was possible, in good agreement with polarizability calculations

using continuum theory.[30–34] To our knowledge, prior to our 2011 publication,[20] a permanent electric field had not been included in the CDM's Hamiltonian, but expressions similar to ours for the electrostatic energy of coupled dipoles in an external electric field have been published before.[35] However, it would appear that the self-consistent dipole-dipole interaction energy between spatially extended particles in an external electric field has not been calculated explicitly yet.

To fit in with our naming scheme, we shall dub the approach that utilizes the CDM the "cluster of self-consistent dipoles" (CSCD) approach. In the case where each "cluster" in fact consists of only one dipole and hence the CDM is applied to only two interacting dipoles, we reserve a separate name and acronym: the "single self-consistent dipoles" (SSCD) approach. The reason for this distinction is that in the special case of two interacting dipoles, the set of linear equations can be solved analytically such that, for the SSCD, we use an analytical expression instead of numerical linear algebra algorithms. We note here that this analytical expression used in the SSCD approach, though it follows naturally from the CDM, has been derived before by Buckingham and Pople when examining the first-order correction to the Clausius-Mossotti relation for an imperfect gas.[36] Further research in this direction seems to have focused on atomic and molecular gases and crystals;[37–47] in this paper, we wish to concentrate on interactions between colloidal particles and compare various methods for calculating their pair interactions.

In this work, we first introduce the CDM in Sec. II and generalize its formulation somewhat to allow for the description of systems split up into chunks of matter that are not necessarily of atomic proportions. Although we provide the tools for calculating VdW interactions, in this paper we concentrate on the results for electric field-induced interactions. In Section III, we discuss the SSCD in some detail. In Sec. IV, we compare our numerical results for the electric field-induced interaction energy for various particle shapes, namely spheres, cubes, rods, and dumbbells, using the various calculation techniques discussed above, i.e., the SPD, CPD, SSCD, and CSCD approach (the latter of which we deem to be the "exact" result if the number of dipoles is large enough). We also vary the number of dipoles per cluster to investigate how many dipoles are required for an accurate description of the interaction energy. We find that the accuracy of the various approaches depends mainly on the degree of anisotropy in the particle shape, with the SSCD approach performing well for spheres and cubes, even better than the CPD approach. For rods, however, both single dipole approaches (SSCD and SPD) are severely lacking in accuracy and the cluster approaches (CSCD and CPD) give better results. Here, an approach that uses clusters of a very small number of self-consistent dipoles turns out to give very good accuracy. As for the question of how many dipoles are sufficient to accurately describe the electric field-induced interaction, we find that the answer depends strongly on the particle shape, with cubes and cuboidal rods generally needing a smaller number of dipoles than spheres do. The reason might be that a spherical shape is hard to approximate using identical chunks whereas, for cubes and cuboidal rods, this is trivial even with a very low number of chunks.

II. THE CDM

In previous work,[17,18,20,29,48] when considering physical systems using the CDM, the atoms are usually modeled as Lorentz atoms: they are assumed to consist of a nucleus and one electron bound to it by a harmonic force. In such a model, the charges making up the induced dipole are $\pm e$, where e is the elementary charge, and the mass of the vibrating part of the atom is the electron mass m_e. If the harmonic force is defined to have the characteristic frequency ω_0, the atomic polarizability then follows by[15,49]

$$\alpha_0 = \frac{e^2}{m_e \omega_0^2}. \tag{1}$$

The Hamiltonian H of a system of N Lorentz atoms in an external electric field $\mathbf{E}_0$ can be written as

$$\begin{aligned} H(\{\mathbf{d}_i\},\{\mathbf{k}_i\}) = {} & \frac{1}{2m_e}\sum_{i=1}^{N}\mathbf{k}_i^2 \\ & + \frac{e^2}{2\alpha_0}\sum_{i=1}^{N}\mathbf{d}_i\cdot(\mathbf{I}\delta_{ij} - \alpha_0\mathbf{T}_{ij})\cdot\mathbf{d}_j \\ & - e\sum_{i=1}^{N}\mathbf{d}_i\cdot\mathbf{E}_0. \end{aligned} \tag{2}$$

Here, $\mathbf{I}$ is the 3×3 identity matrix, $\mathbf{k}_i$ is the momentum of the electron associated with atom i, and $\mathbf{d}_i$ is this electron's distance vector to the atom nucleus. The matrix $\mathbf{T}_{ij}$ is the dipole tensor

$$\mathbf{T}_{ij} = \begin{cases} \left(3\mathbf{r}_{ij}\mathbf{r}_{ij}/r_{ij}^2 - \mathbf{I}\right)/r_{ij}^3 & \text{if } i \neq j, \\ \mathbf{0} & \text{if } i = j, \end{cases}$$

where $\mathbf{r}_{ij} = \mathbf{r}_i - \mathbf{r}_j$, $r_{ij} = |\mathbf{r}_{ij}|$ and $\mathbf{0}$ is a 3×3 matrix filled with zeros. We note here that by a canonical transformation $(\{\mathbf{d}_i\},\{\mathbf{k}_i\}) \to (\{\mathbf{p}_i\},\{\mathbf{k}'_i\})$, where $\mathbf{p}_i = e\mathbf{d}_i$ and $\mathbf{k}'_i = m_e\dot{\mathbf{p}}_i/e^2$, we could write the Hamiltonian (2) such that only the atomic properties α_0 and e^2/m_e would be input parameters. For simplicity, we will continue to use $(\{\mathbf{d}_i\},\{\mathbf{k}_i\})$ as coordinates, but we note that the CDM thus depends on only two atomic properties (α_0 and e^2/m_e).

We wish to model systems where the Lorentz "atoms" in fact represent "chunks" of matter instead of physical atoms. For this purpose, we generalize the three atomic properties: the charge of oscillator i becomes q_i, its mass m_i, and the polarizability becomes $\boldsymbol{\alpha}_i$, which we choose to be a 3×3 tensor in order to allow for anisotropic chunk polarizabilities. In terms of these quantities, the Hamiltonian reads

$$\begin{aligned} H(\{\mathbf{d}_i\},\{\mathbf{k}_i\}) = {} & \frac{1}{2}\sum_{i=1}^{N}\mathbf{k}_i\cdot\mathbf{m}_i^{-1}\cdot\mathbf{k}_i \\ & + \frac{1}{2}\sum_{i=1}^{N}\mathbf{d}_i\cdot\mathbf{q}_i\cdot\left(\boldsymbol{\alpha}_i^{-1}\delta_{ij} - \mathbf{T}_{ij}\right)\cdot\mathbf{q}_j\cdot\mathbf{d}_j \\ & - \sum_{i=1}^{N}(\mathbf{q}_i\cdot\mathbf{d}_i)\cdot\mathbf{E}_0, \end{aligned}$$

where we defined the matrices $\mathbf{m}_i \equiv m_i\mathbf{I}$ and $\mathbf{q}_i \equiv q_i\mathbf{I}$. We now introduce $3N$-dimensional vectors $\mathcal{K}$, $\mathcal{D}$, and $\mathcal{E}_0$, which

are built up out of the $\mathbf{k}_i$, $\mathbf{d}_i$, and copies of $\mathbf{E}_0$, respectively. Furthermore, we define the $3N \times 3N$-dimensional matrices $\mathcal{M} \equiv \text{diag}(\{\mathbf{m}_i\})$, $\mathcal{Q} \equiv \text{diag}(\{\mathbf{q}_i\})$, $\mathcal{A} \equiv \text{diag}(\{\boldsymbol{\alpha}_i\})$, and, lastly, $\mathcal{T}$, built up out of all the $\mathbf{T}_{ij}$. In terms of these quantities, the Hamiltonian reads

$$H(\mathcal{D}, \mathcal{K}) = \frac{1}{2}\mathcal{K} \cdot \mathcal{M}^{-1} \cdot \mathcal{K} + \frac{1}{2}\mathcal{D} \cdot \mathcal{Q} \cdot (\mathcal{A}^{-1} - \mathcal{T}) \cdot \mathcal{Q} \cdot \mathcal{D} - (\mathcal{Q} \cdot \mathcal{D}) \cdot \mathcal{E}_0,$$

and, since all the matrices involved are symmetric, the square can be completed such that

$$H = H_0 + U_E.$$

Here, H_0 is the Hamiltonian of a set of shifted harmonic oscillators,

$$H_0 = \frac{1}{2}\mathcal{K} \cdot \mathcal{M}^{-1} \cdot \mathcal{K} + \frac{1}{2}(\mathcal{D} - \mathcal{D}_0) \cdot \mathcal{Q} \cdot (\mathcal{A}^{-1} - \mathcal{T}) \cdot \mathcal{Q} \cdot (\mathcal{D} - \mathcal{D}_0),$$

with $\mathcal{D}_0$ a (time-independent) $3N$-dimensional vector that describes the shift of the equilibrium positions, satisfying the equation

$$(\mathcal{A}^{-1} - \mathcal{T}) \cdot \mathcal{Q} \cdot \mathcal{D}_0 = \mathcal{E}_0. \tag{3}$$

The constant potential energy shift due to the electric field reads

$$U_E \equiv -\frac{1}{2}\mathcal{E}_0 \cdot (\mathcal{A}^{-1} - \mathcal{T})^{-1} \cdot \mathcal{E}_0. \tag{4}$$

We switched the Hamiltonian variable $\mathcal{D}$ to $\mathcal{D} - \mathcal{D}_0$, which is allowed since $\mathcal{K}$ is also $\mathcal{D} - \mathcal{D}_0$'s conjugate momentum.

The equations of motion that follow from the Hamilton equations can be combined into:

$$\frac{\partial^2(\mathcal{D} - \mathcal{D}_0)}{\partial t^2} = -\mathcal{M}^{-1}\mathcal{Q} \cdot (\mathcal{A}^{-1} - \mathcal{T}) \cdot \mathcal{Q} \cdot (\mathcal{D} - \mathcal{D}_0), \tag{5}$$

which describes oscillatory modes about the shifted equilibrium of the form

$$\mathcal{D} - \mathcal{D}_0 = \mathcal{C}_k \exp[i\Omega_k t], \tag{6}$$

where $\mathcal{C}_k$ is a $3N$-dimensional vector of constants and Ω_k is an angular frequency. Substituting Eq. (6) into Eq. (5), we arrive at the eigenvalue equation

$$\Omega_k^2 \mathcal{C}_k = \mathcal{S} \cdot \mathcal{C}_k, \tag{7}$$

where we defined the $3N \times 3N$ matrix

$$\mathcal{S} \equiv \mathcal{M}^{-1} \cdot \mathcal{Q} \cdot (\mathcal{A}^{-1} - \mathcal{T}) \cdot \mathcal{Q}. \tag{8}$$

Because of the dimensions of $\mathcal{S}$, Eq. (7) has $3N$ solutions labeled by $k = 1, 2, \ldots, 3N$, each corresponding to a mode frequency Ω_k. It is worthwhile to note that it can be shown that the eigenvalues of $\mathcal{S}$ are also the eigenvalues of the symmetric matrix $\mathcal{S}_{sym} = \mathcal{M}^{-1/2} \cdot \mathcal{Q} \cdot (\mathcal{A}^{-1} - \mathcal{T}) \cdot \mathcal{Q} \cdot \mathcal{M}^{-1/2}$, albeit with different eigenvectors. This gives a computational advantage since $\mathcal{S}_{sym}$ is symmetric, whereas $\mathcal{S}$ may not be. As a further note, if we had chosen to use the $(\{\mathbf{p}_i\}, \{\mathbf{k}'_i\})$ coordinate system, we would have obtained $\mathcal{S}' = \mathcal{F} \cdot (\mathcal{A}^{-1} - \mathcal{T})$, or $\mathcal{S}'_{sym} = \mathcal{F}^{1/2} \cdot (\mathcal{A}^{-1} - \mathcal{T}) \cdot \mathcal{F}^{1/2}$, where $\mathcal{F} = \text{diag}(\{\frac{q_i^2}{m_i}\mathbf{I}\})$. Note that $\mathcal{S}'$ and $\mathcal{S}'_{sym}$ have the same eigenvalues as $\mathcal{S}$ and $\mathcal{S}_{sym}$.

As mentioned, the CDM depends on the fractions q_i^2/m_i of the CDM-"atoms." For physical atoms, these quantities could be obtained from ω_0, but if our "atoms" represent multiple physical atoms, it is not *a priori* clear which reasonable value to choose for q_i^2/m_i. In the supplementary material,[50] we argue, using the example of pair interaction between particles in the simplified case where each chunk is identical, that the chunks' characteristic frequency $\omega_d = q_d^2/m_d\alpha_d$ should in fact equal the characteristic frequency ω_0 of the material we wish to model.

From a quantum mechanical point of view, the sum of the normal mode frequencies is the ground-state potential energy U_0 of the Hamiltonian H_0,

$$U_0 = \frac{1}{2}\hbar \sum_{k=1}^{3N} \Omega_k, \tag{9}$$

where $\hbar$ is the reduced Planck constant. This energy U_0 stems from the zero-point motion of the harmonic oscillators and contains the VdW interaction energy of the system.

Re-examining the trial solution of Eq. (6), we note that the equilibrium ("average") electron-nucleus distance is not zero, but $\mathcal{D}_0$. Physically, this means that each chunk's (ground state) electron cloud is shifted by a distance given by its associated 3-dimensional vector contained in $\mathcal{D}_0$, such that the average position of the electrons no longer coincides with their nucleus. This gives rise to an average chunk dipole moment $\mathcal{P} = \mathcal{Q} \cdot \mathcal{D}_0$ that satisfies, from Eq. (3),

$$(\mathcal{A}^{-1} - \mathcal{T}) \cdot \mathcal{P} = \mathcal{E}_0. \tag{10}$$

Thus, in terms of $\mathcal{P}$, the electrostatic energy U_E as defined in Eq. (4) is

$$U_E = -\frac{1}{2}\mathcal{P} \cdot \mathcal{E}_0, \tag{11}$$

which is consistent with the form of the energy of an induced dipole in an electric field; note that the factor $\frac{1}{2}$ arises from the fact that the dipole is induced, not permanent.[15] We can simplify Eq. (11) further by reverting to 3-dimensional vectors:

$$U_E = -\frac{1}{2}\mathbf{p}_{tot} \cdot \mathbf{E}_0,$$

where $\mathbf{p}_{tot}$ is the total polarization of the N chunks:

$$\mathbf{p}_{tot} = \sum_{i=1}^{N} \mathbf{p}_i,$$

where $\mathbf{p}_i$ is the polarization of chunk i. As a final step, we note that, as long as $\mathbf{E}_0$ is spatially homogeneous, it turns out that $\mathbf{p}_{tot}$ can always be written in terms of a 3×3 matrix and the applied electric field:

$$\mathbf{p}_{tot} = \boldsymbol{\alpha} \cdot \mathbf{E}_0.$$

We call the matrix $\boldsymbol{\alpha}$ the polarizability matrix of the atom cluster. Mathematically, it is given by $\boldsymbol{\alpha} = \sum_{ij} \mathbf{B}_{ij}$, where $\mathbf{B}_{ij}$ are 3×3 blocks of the matrix $(\mathcal{A}^{-1} - \mathcal{T})^{-1}$. However, since matrix inversion is computationally more expensive than finding

the solution to a linear system such as Eq. (10), it is in practice more efficient to infer $\boldsymbol{\alpha}$ by calculating the three $\mathbf{p}_{tot}$'s that result from applying the electric field in each of the three Cartesian directions. In terms of $\boldsymbol{\alpha}$, U_E can be written as

$$U_E = -\frac{1}{2}\mathbf{E}_0 \cdot \boldsymbol{\alpha} \cdot \mathbf{E}_0. \tag{12}$$

Closely related to the polarizability matrix is the enhancement factor matrix, which we define as

$$\mathbf{f} = \left(\sum_{i=1}^{N} \boldsymbol{\alpha}_i\right)^{-1} \boldsymbol{\alpha}.$$

The enhancement factor quantifies the influence of chunk-chunk interactions on the overall polarizability, since $\sum_{i=1}^{N} \boldsymbol{\alpha}_i$ is the polarizability one would expect if one were to ignore these interactions. Note that if each chunk has the same isotropic polarizability $\boldsymbol{\alpha}_i = \alpha_0 \mathbf{I}$, the enhancement factor reduces to $\boldsymbol{\alpha}_i / N\alpha_0$, which is the familiar expression used in Refs. 19, 20, and 29.

A. Interactions between particle pairs

The energies U_0 and U_E of Eqs. (9) and (12) are total potential energies and, thus, contain the interactions between all atoms, including each atom's self-energy, i.e., the energy that the atom would have if there were no other atoms in the system. In this work, we are mainly interested in interactions between colloidal particles, which we treat as clusters of atoms. To obtain the interaction energy between two clusters of atoms, we calculate, for a given separation and orientation of the clusters, the total potential energies U_0 and U_E and subsequently subtract the energy that the clusters would have if their separation were infinite. This is equivalent to subtracting each cluster's self-energy, i.e., the cluster's energy as if there were no other clusters. We can write the two-cluster interaction energy $V_E^{(2)}$ as[48]

$$V_E^{(2)} = U_E^{(2)} - U_{E,1}^{(1)} - U_{E,2}^{(1)},$$

$V_0^{(2)}$ has a similar expression. Here, $U_E^{(2)}$ is the total potential energy of this system of two clusters of atoms and $U_{E,1}^{(1)}$ and $U_{E,2}^{(1)}$ are the self-energy of cluster 1 and 2, respectively. In this work, we only consider pair interactions and intend to compare the results of various calculation techniques. For clarity, we therefore now modify the notation somewhat, so that the pair interaction between clusters of atoms with self-consistent dipole moments will from now on be referred to as $V_{0,X}^{(\mathrm{CSCD})}$ (for VdW) and $V_{E,X}^{(\mathrm{CSCD})}$ (for electric field-induced interaction), where we replace "X" by the cluster type that we are considering (i.e., "sphere", "cube," or "rod"). The pair interaction in the special case where the "clusters" of atoms in fact consist of only one atom each, is denoted by $V_0^{(\mathrm{SSCD})}$(for VdW) and $V_E^{(\mathrm{SSCD})}$ (for electric field-induced interaction). The acronym in the superscript refers to the method of calculation. In the results presented in this work, we only consider the electrostatic interaction energy V_E. An outline of how the VdW interaction V_0 can be calculated using the CDM is given in the supplementary material.[50]

We now discuss some more assumptions and notation that will be used in the remainder of this paper and in the supplementary material.[50] The interaction energy between pairs of particles will be investigated as a function of the relative position of the second particle with respect to the first. This relative position can either be expressed as polar coordinates, where r is the center-to-center distance between the particles and θ is the angle between the applied electric field $\mathbf{E}_0$ and the line connecting the particle centers, or as Cartesian coordinates, where $r_\parallel$ is the position along the direction of the electric field and $r_\perp$ is the position along the direction perpendicular to it. Note that we only consider two dimensions.

In this work, we only consider pairs of identical particles, although, for rods and cubes, we do consider a case where one particle is rotated with respect to the other. When modeling the particles as clusters of multiple Lorentz atoms ("chunks"), we only consider modeling schemes where all Lorentz atoms are identical and have an isotropic polarizability $\boldsymbol{\alpha}_d = \alpha_d \mathbf{I}$, with α_d a scalar constant. The number of Lorentz atoms per cluster is indicated by $N_{d/p}$. The value of α_d is determined by assigning a certain scalar "target" polarizability α_p to the cluster. The chunk polarizability α_d is then tuned such that the cluster's actual polarizability α_c is very close to α_p; i.e., we find the root of the function $\alpha_c(\alpha_d) - \alpha_p$ by using Ridder's bracketing algorithm.[51] In the special case where each cluster consists of only one Lorentz atom, we can instead simply set $\alpha_d = \alpha_p$. We note that only isotropically polarizable particles have a scalar polarizability; for rods and dumbbells (which do not have an isotropic polarizability), α_p and α_c are chosen to correspond to the polarizability along the particle's "long" Cartesian axis.

The electrostatic interaction energy depends only on the inverse of the matrix $(\mathcal{A}^{-1} - \mathcal{T})$. This inverse can in principle be calculated analytically for any number of dipoles, but this calculation already becomes infeasible when the number of dipoles exceeds two. Therefore, if the number of dipoles per particle $N_{d/p} > 1$, we solve Eq. (10) numerically for $\mathcal{P}$ and take its inner product with $\mathcal{E}_0$ [Eq. (11)] (this circumvents having to calculate $\boldsymbol{\alpha}$). On the other hand, if each particle is modeled as a single dipole ($N_{d/p} = 1$), we can simply insert $\alpha_d = \alpha_p$ into the analytical expressions of Section III.

III. INTERACTION BETWEEN A PAIR OF IDENTICAL LORENTZ ATOMS

For two Lorentz atoms in the electric field $\mathbf{E}_0$, the potential energy, as calculated from Eq. (12), is

$$U_E^{(\mathrm{SSCD})} = \alpha_d E_0^2 \frac{\tilde{r}^3(-\tilde{r}^3 + 2 - 3\cos^2\theta)}{(\tilde{r}^3 - 2)(\tilde{r}^3 + 1)},$$

where $\tilde{r} = r/\alpha_d^{1/3}$ is the dimensionless distance between the dipoles. This expression is equivalent to the one derived in Ref. 36. The energy at infinite separation is $-\alpha_d E_0^2$, which is reasonable physically, since both particles in this case are induced dipoles with dipole moment $\alpha_d E_0$ and, thus, they each have energy $-\frac{1}{2}\alpha_d E_0^2$. Subtracting the energy at infinite separation from U_E, we arrive at the interaction energy

$$V_E^{(\mathrm{SSCD})}(\tilde{r}, \theta) = \alpha_d E_0^2 \frac{\tilde{r}^3 - 2 - 3\tilde{r}^3\cos^2\theta}{(\tilde{r}^3 - 2)(\tilde{r}^3 + 1)}. \tag{13}$$

This is the self-consistent interaction energy between a pair of Lorentz atoms in an external electric field where, by "self-consistent," we mean that the dipoles have a dipole moment equal to their polarizability α_d multiplied by the local electric field (the external electric field plus the electric field due to the other dipole). A simpler and more commonly used approach to calculating the interaction energy of two Lorentz atoms in an electric field is to impose upon each atom a "permanent dipole" moment $\alpha_d \mathbf{E}_0$ and use this setup to calculate the well-known dipole-dipole interaction energy,[15] resulting in

$$V_E^{(\mathrm{SPD})}(\tilde{r},\theta) = \alpha_d E_0^2 \frac{1-3\cos^2\theta}{\tilde{r}^3}. \tag{14}$$

As it turns out, $V_E^{(\mathrm{SPD})}(\tilde{r},\theta)$ is the first-order approximation of $V_E^{(\mathrm{SSCD})}(\tilde{r},\theta)$ for small $\tilde{r}^{-3}$: Taylor expanding Eq. (13) yields

$$\frac{V_E^{(\mathrm{SSCD})}(\tilde{r},\theta)}{E_0^2\alpha_d} \simeq \frac{V_E^{(\mathrm{SPD})}(\tilde{r},\theta)}{E_0^2\alpha_d} - \frac{1+3\cos^2\theta}{\tilde{r}^6} + \mathcal{O}([\tilde{r}^{-3}]^3).$$

We note that the first correction term is always negative, indicating that $V_E^{(\mathrm{SSCD})}(\tilde{r},\theta)$ has a larger attractive region than $V_E^{(\mathrm{SPD})}(\tilde{r},\theta)$. Indeed, the angle $\theta_0^{(\mathrm{SSCD})}$ at which $V_E^{(\mathrm{SSCD})}(\tilde{r},\theta_0^{(\mathrm{SSCD})}) = 0$ is given by

$$\theta_0^{(\mathrm{SSCD})}(\tilde{r}) = \arccos\sqrt{\frac{\tilde{r}^3-2}{3\tilde{r}^3}},$$

whereas this angle for $V_E^{(\mathrm{SPD})}(\tilde{r},\theta)$ is the limit $\theta_0^{(\mathrm{SSCD})}(\tilde{r} \to \infty)$, which is the well-known "magic" angle $\theta_0^{(\mathrm{SPD})} = \arccos\sqrt{1/3} \approx 54.7^\circ$. We note that $\theta_0^{(\mathrm{SSCD})}(\tilde{r})$ increases as $\tilde{r}$ decreases, with as limiting value $\theta_0^{(\mathrm{SSCD})}(\tilde{r} \to 2^{1/3}) = \pi/2$, indicating an attractive interaction for all angles except $\pi/2$. This limiting case coincides with the occurrence of the "polarization catastrophe": $V_E^{(\mathrm{SSCD})}(\tilde{r} \to 2^{1/3},\theta)$ diverges for all θ except $\theta = \theta_0^{(\mathrm{SSCD})}$ (in which case the limiting value is $\alpha_d E_0^2/3$). We deem the values produced by $V_E^{(\mathrm{SSCD})}$ for $\tilde{r} \le 2^{1/3}$ unphysical. A further difference between $V_E^{(\mathrm{SSCD})}(\tilde{r},\theta)$ and $V_E^{(\mathrm{SPD})}(\tilde{r},\theta)$ is the relative strength of the attraction and repulsion for $\theta = 0$ and $\theta = \pi/2$. The ratio between these two is a constant in the SPD approach, $V_E^{(\mathrm{SPD})}(\tilde{r},0)/V_E^{(\mathrm{SPD})}(\tilde{r},\pi/2) = -2$, but in the self-consistent (SSCD) case it is given by

$$\frac{V_E^{(\mathrm{SSCD})}(\tilde{r},0)}{V_E^{(\mathrm{SSCD})}(\tilde{r},\pi/2)} = -2\frac{\tilde{r}^3+1}{\tilde{r}^3-2}. \tag{15}$$

For large distances, Eq. (15) goes to the constant -2, while for $\tilde{r} \to 2^{1/3}$ it goes to $-\infty$, which reflects the fact that $V_E^{(\mathrm{SSCD})}(\tilde{r} \to 2^{1/3},0)$ diverges but $V_E^{(\mathrm{SSCD})}(\tilde{r} \to 2^{1/3},\pi/2)$ does not.

Figure 1 is a contour plot of $V_E^{(\mathrm{SSCD})}(\tilde{r},\theta)$ as a function of the location of the second dipole, with the first being kept at the origin. Also plotted in the same figure are the contours of $V_E^{(\mathrm{SPD})}(\tilde{r},\theta)$, as well as the line denoting the 54.7° magic angle. In this case, trivially, the $V_E^{(\mathrm{SPD})}(\tilde{r},\theta) = 0$ contour coincides with this line. We see that for small separation, the $V_E^{(\mathrm{SPD})}(\tilde{r},\theta)$ contours are very different in shape and location

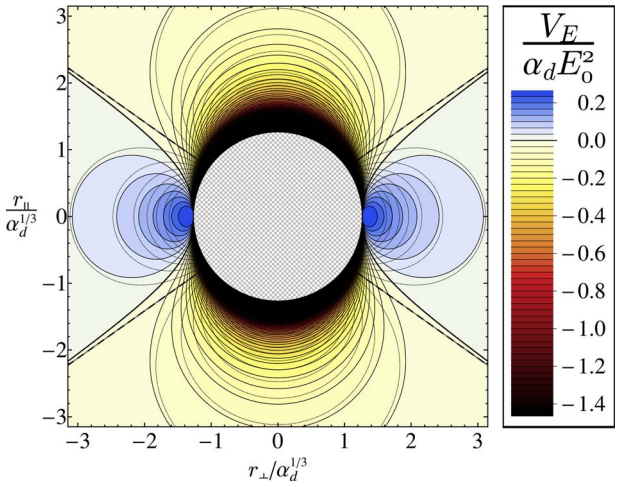

FIG. 1. Contour plot of the interaction energy $V_E^{(\mathrm{SSCD})}/\alpha_d E_0^2$, as given in Eq. (13), of a pair of Lorentz atoms with polarizability α_d subject to an external electric field $\mathbf{E}_0$ that points along $r_\parallel$ (the vertical axis of the plot), as a function of the location $(r_\perp, r_\parallel)$ of the second Lorentz atom. The dipole moments are calculated self-consistently (see text). The contour lines of the function $V_E^{(\mathrm{SPD})}/\alpha_d E_0^2$ of Eq. (14), which is the result of the single permanent dipole (SPD) approach where each dipole has a fixed dipole moment equal to $\alpha_d \mathbf{E}_0$, are shown as see-through lines. The hatched area is excluded from the plot: at distances $r/\alpha_d^{1/3} \le 2^{1/3} \approx 1.26$, a polarization catastrophe occurs and $V_E^{(\mathrm{SSCD})}(\tilde{r},\theta)/\alpha_d E_0^2$ is no longer valid.

than their $V_E^{(\mathrm{SSCD})}(\tilde{r},\theta)$ counterparts. For large separation, the contours start to coincide more, as expected, since the first-order approximation dominates the Taylor series for large distances.

It is also possible to analytically calculate the interaction energy of particles with anisotropic polarizability. The simplest example of such particles are particles with a diagonal polarizability matrix with only two independent entries, α_{xx} and α_{zz}. All particles with at least a 4-fold rotational symmetry axis have a polarizability of this form; examples include rods, dumbbells, platelets, and bowls.[20] In the following, we assume that the electric field is pointing in the z-direction and that both particles are perfectly aligned with it. Thus, the Cartesian coordinate system is defined by the electric field direction and not the symmetry axis of the particles. In fact, rods and dumbbells align their rotational symmetry axis along the electric field (i.e., in the z-direction), whereas bowls and platelets align their rotational symmetry axis perpendicular to the electric field (i.e., in the x-y plane),[20] meaning that for rods and dumbbells, $\alpha_{yy} = \alpha_{xx}$, but for bowls and platelets, $\alpha_{yy} = \alpha_{zz}$. However, as the value of α_{yy} turns out to be irrelevant for the mathematical expression of the interaction energy, the result is valid in both cases. Keeping the first particle at the origin and parametrizing the position of the second by the distance r and the polar angle θ (the angle between the electric field and the line connecting the particles), the interaction energy is

$$V_{E,\,\mathrm{anistropic}}^{(\mathrm{SSCD})}(\tilde{r},\theta,\eta_\alpha) = E_0^2\alpha_{zz}\frac{(\tilde{r}^3-2\eta_\alpha-3\tilde{r}^3\cos^2\theta)}{(\tilde{r}^3+1)(\tilde{r}^3-2\eta_\alpha)-3(1-\eta_\alpha)\tilde{r}^3\cos^2\theta}, \tag{16}$$

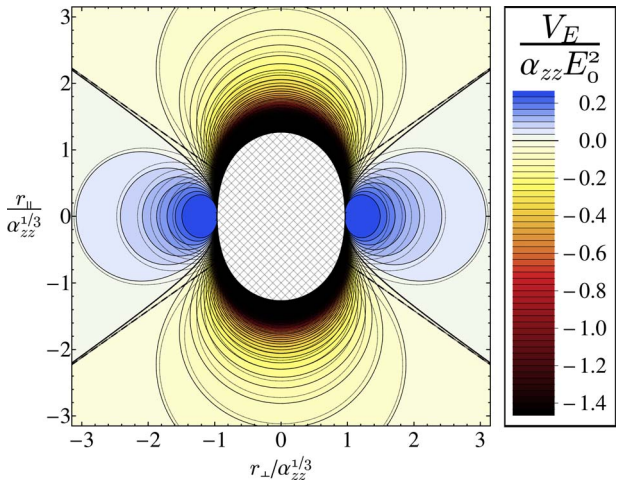

FIG. 2. Contour plot of the interaction energy $V_E^{(\mathrm{SSCD})}/\alpha_{zz}E_0^2$, as given in Eq. (16), of a pair of Lorentz atoms, each with anisotropic polarizability $\boldsymbol{\alpha}_d = \mathrm{diag}(\alpha_{xx}, \alpha_{yy}, \alpha_{zz})$ satisfying $\alpha_{xx}/\alpha_{zz} = 0.44$, subject to an external electric field $\mathbf{E}_0$ pointing in the z-direction, as a function of the location of the second Lorentz atom relative to the first in the x-z plane. Note that restricting ourselves to this plane makes the value of α_{yy} irrelevant for $V_E^{(\mathrm{SSCD})}$. The dipole moments are calculated self-consistently (see text). The contour lines (see-through) of the function $V_E^{(\mathrm{SPD})}/\alpha_d E_0^2$ of Eq. (14), which is the result of the single permanent dipole (SPD) approach where each dipole has a fixed dipole moment equal to $\alpha_{zz}\mathbf{E}_0$, are shown as well. The hatched area, within which a polarization catastrophe occurs and $V_E^{(\mathrm{SSCD})}$ is no longer valid, is excluded from the plot.

where $\tilde{r} = r/\alpha_{zz}^{1/3}$ and $\eta_\alpha = \alpha_{xx}/\alpha_{zz}$, which always satisfies $\eta_\alpha < 1$. This function is plotted for $\eta_\alpha = 0.44$ in Fig. 2, along with the contours of its first-order approximation, which equals $V_E^{(\mathrm{SPD})}(\tilde{r}, \theta)$ with $\alpha_d = \alpha_{zz}$. Here, the choice of $\eta_\alpha = 0.44$ was made because it coincides with the observed η_α of the particular (cuboidal) rod-shaped particles that we consider in this work.[50] The plot looks similar to the one that was shown in Fig. 1, albeit squished together along the horizontal ($r_\perp$-)axis.

IV. INTERACTION BETWEEN CLUSTER PAIRS

We now proceed to numerically calculate the induced-dipole interaction energy between pairs of clusters of atoms, which we model to represent micron-sized particles. Before presenting results, we discuss the applied methods in practical terms, which are the same for each cluster shape we consider. In the body of this paper, we include detailed numerical results for spheres but, for brevity, we leave out the details for cuboidal and spherocylindrical rods, cubes, dumbbells, and misaligned particles. A more detailed discussion can be found in the supplementary material.[50]

A. Methods

To infer the positions of the dipole chunks, we first decide on a desired particle size, the number of dipole chunks $N_{d/p}$ we will use to model each particle, and the lattice type to arrange the dipole chunks on. We then infer the lattice spacing a of the dipoles to determine the positions of the dipoles. Then we proceed to tune the dipoles' polarizability α_d such that the polarizability α_c of the cluster of dipoles is close to the desired polarizability α_p of the particle we wish to model.

In choosing the polarizability α_p, it is important to beware of the polarization catastrophe. As α_d increases, the dimensionless lattice spacing $\tilde{a} = a/\alpha_d^{1/3}$ decreases, and α_c increases until, for a certain $\tilde{a}$, the polarization catastrophe occurs, with α_c diverging into a $(\tilde{a} - \tilde{a}_{\mathrm{cat}})^{-1}$-like peak, where $\tilde{a}_{\mathrm{cat}}$ is the dimensionless lattice spacing at which the polarization catastrophe occurs. For $\tilde{a} < \tilde{a}_{\mathrm{cat}}$, the function α_c is characterized by many of these divergences, with ranges between the divergences where α_c seems well-behaved but where the values for computed physical quantities such as $V_E^{(2)}$ cannot be trusted. Another point of interest is that the exact value of $\tilde{a}_{\mathrm{cat}}$ is dependent on the number of dipoles in the system and their arrangement with respect to each other. Therefore, even though the first divergence in theory makes it possible to create a cluster of dipoles with an arbitrarily high cluster polarizability (by choosing an α_d such that $\tilde{a}$ is only just above $\tilde{a}_{\mathrm{cat}}$), when two of these clusters are allowed to interact, $\tilde{a}_{\mathrm{cat}}$ may increase, such that the system's dimensionless lattice spacing becomes $\tilde{a} < \tilde{a}_{\mathrm{cat}}$. This could easily remain unnoticed, since α_c is well-behaved between its divergences, but the numerical results are not reliable in this case. Therefore, it is prudent to choose α_c such that the resulting α_d is low enough and, thus, $\tilde{a}$ is high enough to be comfortably above $\tilde{a}_{\mathrm{cat}}$.

Having thus determined the properties of the dipoles and the lattice, we place a copy (or, in the case of the misaligned clusters, a rotated copy; these are discussed in Subsection IV C and, in more detail, in the supplementary material[50]) of the cluster at a certain relative position of the cluster and numerically compute the total electrostatic potential energy $U_E^{(2)}$ and each cluster's self-energy $U_{E,1}^{(1)}$ and $U_{E,2}^{(1)}$ (these are equal in the case of identical clusters that are not rotated with respect to each other), and subtract this from $U_E^{(2)}$ to gain the interaction energy $V_E^{(\mathrm{CSCD})}$ at that relative position. We then modify the relative position to calculate a new $V_E^{(\mathrm{CSCD})}$, and repeat this process until the desired sample points have been run through. To generate a contour plot, we additionally have to interpolate in order to gain approximate values for locations between sample points. This occasionally creates slight artefacts in the plots and so, generally, features in the plots smaller than the distance between the sample points should be ignored. The interpolation method is always a 2nd-order spline, chosen because it smooths out the function the best (judged by eye).

We can contrast the CDM's self-consistent manner (i.e., the CSCD approach) of calculating the induced-dipole interaction energy with the more usually applied method, in which each dipole is assigned a permanent moment $\mathbf{p}_d = \alpha_p \mathbf{E}_0/N_{d/p}$, and the total interaction energy can be calculated by summing over pairs of dipoles that are not in the same cluster:

$$V_E^{(\mathrm{CPD})} = \frac{\alpha_p^2 E_0^2}{N_{d/p}^2} \sum_{(ij)} \frac{1 - 3\cos^2\theta_{ij}}{r_{ij}^3}, \tag{17}$$

where r_{ij} is the length of the vector $\mathbf{r}_{ij} = (\mathbf{r}_i - \mathbf{r}_j)$, θ_{ij} is the angle between $\mathbf{r}_{ij}$ and $\mathbf{E}_0$, and the sum, as mentioned, is assumed to run over the appropriate pairs (there are $N_{d/p}^2/2$ of these pairs).

Another method (for spherocylinders and dumbbells) that we will test the accuracy of is the "double charge" (DC) method. In this method, we place near the two ends of the particle a positive and a negative point charge $\pm q$, dependent on their separation $\mathbf{s}$ by the restriction $q\mathbf{s} = \boldsymbol{\alpha}_c \cdot \mathbf{E}_0$, i.e., they form a dipole with a dipole moment equal to the dipole moment that the particle would have if modeled using the CDM. The interaction energy between a pair of particles can then be obtained by simply summing the Coulomb interactions between the charges. We tune the separation $\mathbf{s}$ between the charges (while simultaneously tuning the charge magnitudes such that the dipole moment they form remains the same) to gain the best possible results.

In Subsection IV B, as well as in Subsection IV C and the Supplementary Material,[50] we will be comparing numerical results of various methods of calculation. Apart from qualitative comparisons, we also wish to compare the methods in a quantitative way. Suppose we wish to compare a numerically computed function $g(r_\perp, r_\parallel)$ to another function $h(r_\perp, r_\parallel)$. We can then define a relative deviation

$$\sigma[g,h] = \sqrt{\frac{\int_S d\mathbf{r}[g(r_\perp, r_\parallel) - h(r_\perp, r_\parallel)]^2}{\int_S d\mathbf{r}[h(r_\perp, r_\parallel)]^2}}, \tag{18}$$

where S is some integration area and $d\mathbf{r} = dr_\perp dr_\parallel$ is an infinitesimal area element, as a measure of how "wrong" g is, compared to h. If g is very close to h for all locations in S, $\sigma[g, h]$ will be much smaller than unity, whereas $\sigma[g, h]$ will be of the order of unity or greater if g is off by amounts that are of the same order as h itself. Of course, $\sigma[g, h]$ has some limitations, such as the fact that, even if g is wrong in only a small area, it may still receive a high $\sigma[g, h]$ if its discrepancy in this area is large enough. Also, $\sigma[g, h]$ does not work well if h has divergences that g does not. For example, if S is taken to be an infinite plane of which a disk of radius R around the origin is excluded, $\sigma[V_E^{(\mathrm{SPD})}, V_E^{(\mathrm{SSCD})}]$ goes to unity as $R/\alpha_d^{1/3} \downarrow 2^{1/3}$. We can therefore not use σ to compare $V_E^{(\mathrm{SSCD})}$ and $V_E^{(\mathrm{SPD})}$, because the obtained value would depend strongly on R. However, most of the results that follow do not contain such divergences, such that σ is a useful comparison tool.

As a final remark before moving on to the numerical results, we note that even though, from the theory, $\alpha_p E_0^2$ is a naturally occurring unit of measure for V_E, we have chosen to measure the interaction energy in the familiar units of $k_B T$ at room temperature ($T = 293$ K) instead, and have chosen specific experimental parameters, including an electric field strength of $E_0 = 300$ V mm^{-1}, in order to gain numerical values for the energy. Since V_E is exactly quadratic in E_0, the obtained numbers can be straightforwardly adapted to other electric field strengths. Moreover, we note that V_E is an extensive quantity, that is, if we multiply all distances by a value $\lambda^{1/3}$ and, simultaneously, the polarizability of the particles α_p by λ, the resulting interaction potential is scaled by the same factor. To see this, we note that the polarizability of the system is $\boldsymbol{\alpha} = N\alpha_d \mathbf{f}(\{\mathbf{r}_i/\alpha_d^{1/3}\})$, where $\mathbf{f}$ is the enhancement factor of the system, only dependent on the dimensionless coordinates $\{\mathbf{r}_i/\alpha_d^{1/3}\}$ of the Lorentz atoms. Multiplying the dipole chunk polarizability α_d by λ and the coordinates $\mathbf{r}_i$ by $\lambda^{1/3}$, we note that the dimensionless coordinates, and hence the enhancement factor of the system, remain invariant. Less trivially, we note that the enhancement of each individual particle (cluster of dipole chunks) also remains the same, such that we must have $\alpha_p \propto \alpha_d$ (for constant $\{\mathbf{r}_i/\alpha_d^{1/3}\}$). We note that our scaling scheme has kept the polarizability per unit volume of the particles constant. A less trivial dependence appears when we scale α_p or the dimensions of the particle individually. In general, we can say that the lower the particles' polarizability per unit volume, the closer the CSCD interaction energy gets to the CPD interaction energy, which scales quadratically in α_p.

B. Numerical results for spheres

For spheres of diameter l, we put the dipoles on a face-centered cubic (fcc) lattice and remove any dipoles that are more than a distance $l/2$ away from the origin. If $N_{d/p}$ is large enough, this will produce an approximately spherical cluster shape, while if it is smaller, the resulting cluster will be more faceted. In Fig. 3(a), we plot the interaction energy $V_{E,\mathrm{sphere}}^{(\mathrm{CSCD})}$ between a pair of spheres as a function of the position of the second sphere, with the first being kept at the origin. The spheres have a diameter $l = 1$ μm and a polarizability $\alpha_p = 0.1$ μm^3. The number of dipoles in each sphere is $N_{d/p} = 959$ (i.e., there are 1918 dipoles in the system), the electric field is $E_0 = 300$ V mm^{-1}, and the energy is scaled with the thermal energy at room temperature ($T = 293$ K). In Table I, we give the maximum and minimum of the interaction energy for the various approaches, and also give the relative deviation σ of each approach compared to the CSCD approach. As integration area for σ, we use a disk of radius $2.075l$ (which is also the plotted range), with an excluded region that is a disk of radius l around the origin.

In Fig. 3(b), we plot the single self-consistent dipole potential $V_E^{(\mathrm{SSCD})}$, while the contour lines of $V_{E,\mathrm{sphere}}^{(\mathrm{CSCD})}$ are shown in the same plot. We note that the single-dipole approximation $V_E^{(\mathrm{SSCD})}$ is remarkably accurate, especially at angles perpendicular to the electric field. The accuracy also increases with the distance between the spheres, a distance of $2l$ already exhibiting an excellent agreement for all angles. The approximation is worst near the zero-contour, i.e., the boundary between the attractive and repulsive regions of the plot. While both calculation methods predict a θ_0 greater than the magic angle of 54.7° (also denoted in the plot), the $V_E^{(\mathrm{SSCD})}$ result seems to consistently underestimate θ_0, its zero-contour at contact being about halfway between the zero-contour of $V_{E,\mathrm{sphere}}^{(\mathrm{CSCD})}$ and the 54.7°-line. From Table I, we see that the SSCD approach gives a good approximation for the maximum repulsion but underestimates the maximum attraction strength.

In Fig. 3(c), we judge the accuracy of $V_E^{(\mathrm{SPD})}$ by plotting it together with the contour lines of $V_{E,\mathrm{sphere}}^{(\mathrm{CSCD})}$. We note that the contour lines of $V_E^{(\mathrm{SPD})}$ coincide less well with those of $V_{E,\mathrm{sphere}}^{(\mathrm{CSCD})}$ than do the contour lines of $V_E^{(\mathrm{SSCD})}$ in every region of the plot. From Table I, we see that the SPD approach underestimates attractions even more than the SSCD does, while also overestimating repulsions. Its σ-value is almost a factor 2 higher than that of the SSCD approach.

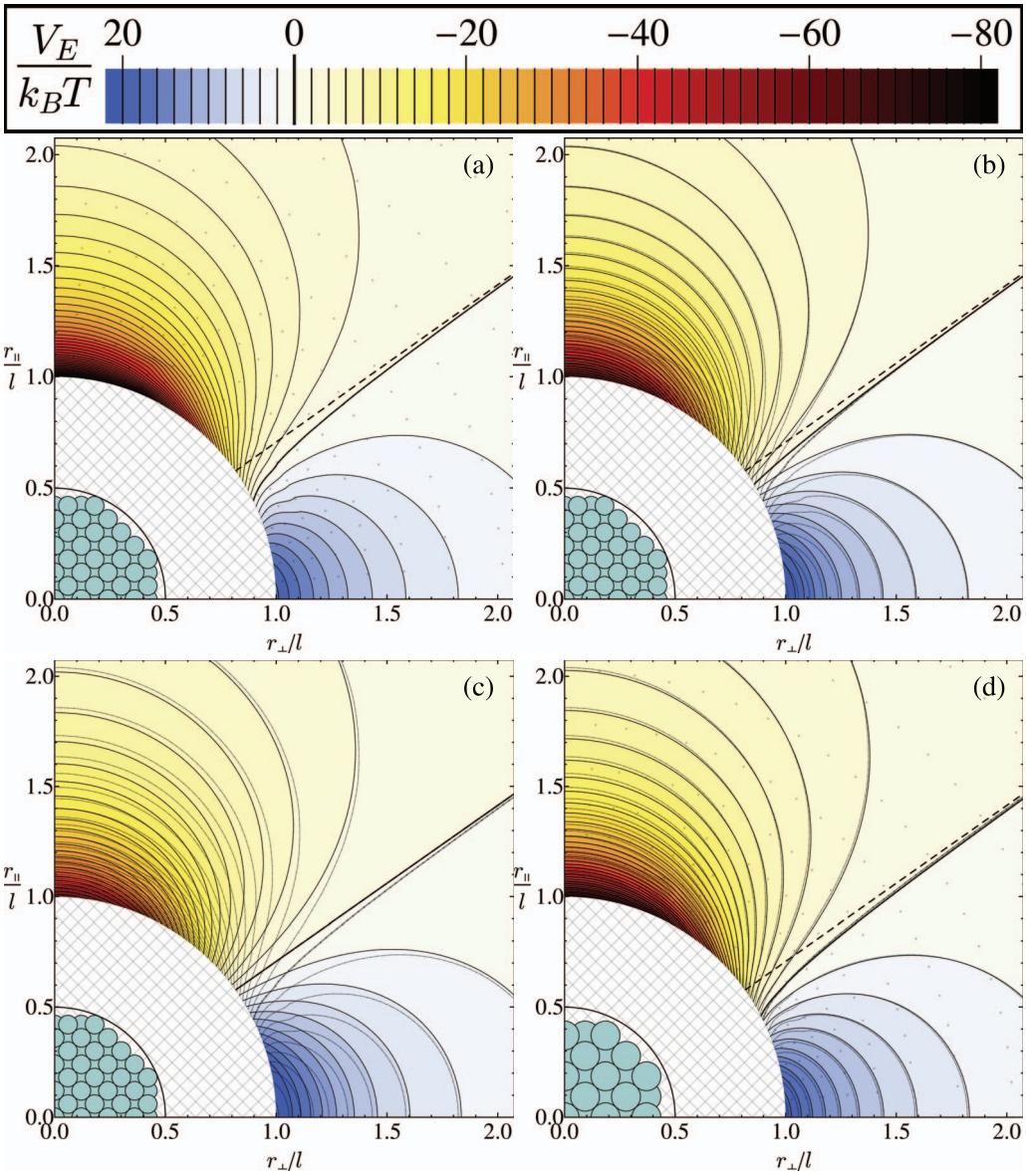

FIG. 3. The interaction energy V_E/k_BT, at $T = 293$ K, of spherical particles with diameter $l = 1$ μm and polarizability $\alpha_p = 0.1$ μm^3, in an external electric field $E_0 = 300$ V mm^{-1} along the $r_\parallel$-axis, as a function of the location of the second particle with respect to the first, calculated using (a) CSCD with 959 dipole chunks per sphere, (b) SSCD, (c) SPD, and (d) CSCD with 225 dipole chunks per sphere (each approach is discussed in the text). Each plot uses the same contour lines and color coding provided in the legend. The dashed lines represent the 54.7° "magic angle." The contour lines of (a) are reproduced as see-through lines in panels ((b)-(d)). A cross-section of the 959-chunk sphere is displayed in the center of panels ((a)-(c)), and that of a 225-chunk sphere in panel (d). The hatched area, within which the spheres overlap, is excluded from the plots. The dots in panels (a) and (d) represent the sample points at which the interaction energy was explicitly calculated.

Next, we compare our calculations using $N_{d/p} = 959$ spheres with those using $N_{d/p} = 225$ spheres. In Fig. 3(d), we plot $V_{E,\text{sphere}}^{(\text{CSCD})}$ for $N_{d/p} = 225$, while showing the contours of $V_{E,\text{sphere}}^{(\text{CSCD})}$ with $N_{d/p} = 959$ in the same figure. We see that the agreement is in general very good for large distances and depends on θ. The agreement is bad for $\theta = 0$ at close distances but improves as θ increases, with the best agreement at roughly $\theta \approx \pi/4$ for close distances and $\theta \approx \pi/6$ for large distances. For values of θ beyond the zero-contour, the agreement gradually deteriorates again but remains much better than the $\theta = 0$ case at close distance. This approach yields a σ-value that is about half of that of the SSCD approach, but still underestimates attractions.

When we compare $V_{E,\text{sphere}}^{(\text{CPD})}$ to the single permanent dipole approximation $V_E^{(\text{SPD})}$, it turns out that, perhaps surprisingly, the contours coincide so well that it makes more sense to show the comparison by a difference plot $(V_{E,\text{sphere}}^{(\text{CPD})} - V_E^{(\text{SPD})})$, which is done in Fig. 4. For the experimental values chosen, the difference between $V_{E,\text{sphere}}^{(\text{CPD})}$ and $V_E^{(\text{SPD})}$ is much smaller than k_BT for all values of r and θ, and $\sigma[V_E^{(\text{SPD})}, V_{E,\text{sphere}}^{(\text{CPD})}] \approx 0.00095$. This implies that modeling a sphere by a number of dipoles and using the permanent dipole approximation to calculate the interaction energy is equivalent to simply modeling it as one dipole, i.e., using $V_E^{(\text{SPD})}$. We note, though, that both approximations are more or less wrong, depending on r and θ, and that $V_E^{(\text{SSCD})}$ is a

TABLE I. Numerical quantities associated with the various calculation techniques for the interaction energy between two spheres, as plotted in Fig. 3. $V_{E,min}$ and $V_{E,max}$ refer, respectively, to the minimum and maximum value achieved by the calculation technique mentioned in the leftmost column. σ is the relative deviation, as defined in Eq. (18), where h is always $V_{E,\text{sphere}}^{(\text{CSCD})}$ and g is the V_E associated with the technique given in the leftmost column. The last entry, "CSCD(225)," refers to the CSCD approach with spheres composed of 225 dipole chunks each, instead of 959.

	σ	$\frac{V_{E,min}}{k_BT}$	$\frac{V_{E,max}}{k_BT}$
CSCD	0	−81.2	20.5
SSCD	0.15	−61.8	22.5
SPD	0.28	−49.4	24.7
CSCD(225)	0.086	−67.12	21.3

better approximation than both, while it is only slightly more complicated to compute than $V_E^{(\text{SPD})}$.

For further illustration, we also plot $V_{E,\text{sphere}}^{(\text{CSCD})}$ and $V_{E,\text{sphere}}^{(\text{CPD})}$ as a function of θ for various r in Fig. 5(a), and as a function of r for various θ in Fig. 5(b). We again note the bad agreement for small distances; e.g., from Fig. 5(a), we see that at contact and at $\theta = 0$, $V_{E,\text{sphere}}^{(\text{CPD})}$ underestimates the interaction energy by about a factor 1.6, corresponding to about $30k_BT$ for the experimental values used. $V_{E,\text{sphere}}^{(\text{CPD})}$ also underestimates the angle at which the crossover from attraction to repulsion occurs, as noted before. The agreement becomes better as the distance increases, as evident by the curves coinciding more and the crossover being more localized to 54.7° in the inset graph. In Fig. 5(b), the interaction energy is plotted as a function of r for $\theta = 0, 0.3\pi$ (an angle close to the magic angle) and 0.5π. As expected, $V_{E,\text{sphere}}^{(\text{CPD})}$ at $\theta = 0.3\pi$ is almost exactly zero for all distances, whereas its $V_{E,\text{sphere}}^{(\text{CSCD})}$ counterpart displays a significant attraction for close distances, up to roughly $14k_BT$.

In conclusion, for spheres, it seems unnecessary to use the SPD (or CPD) approach, since the SSCD approach gives a better result and is not (significantly) more expensive computationally. The CSCD approach with 225 polarizable chunks per sphere gives a better approximation than the SSCD approach but is also more computationally expensive and still

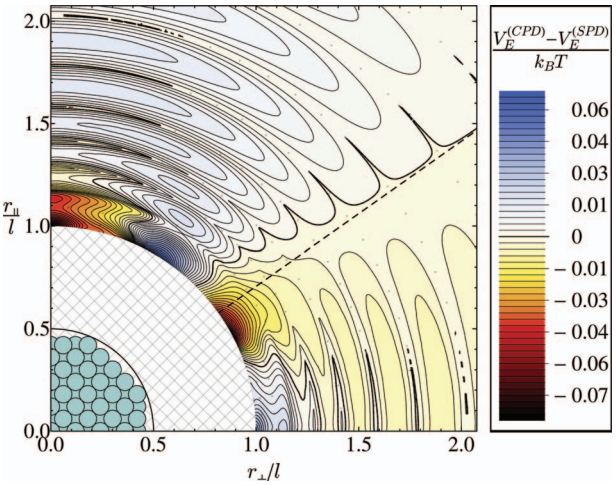

FIG. 4. A comparison of the SPD and CPD approaches for calculating the sphere interaction energy of Fig. 3. Plotted is the difference between the CPD and the SPD result, in units of k_BT.

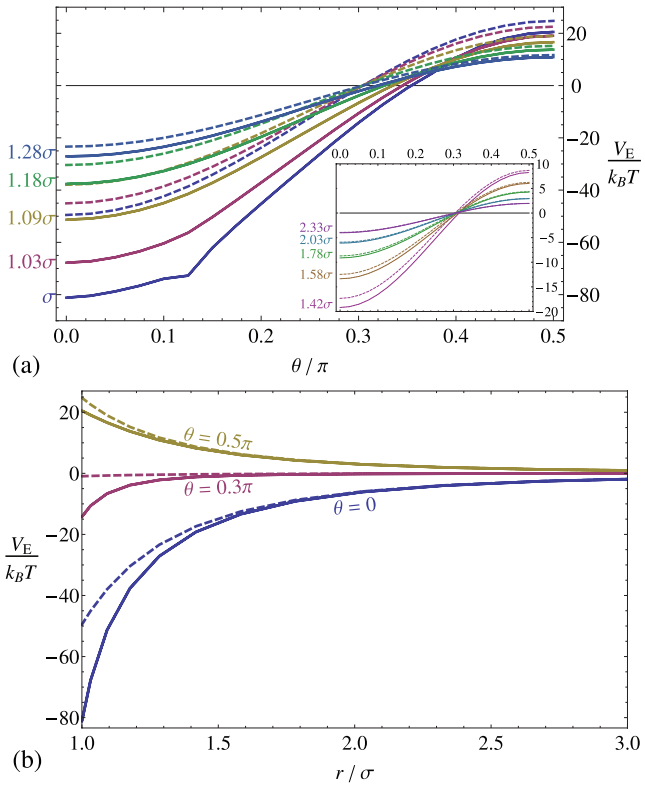

FIG. 5. The sphere interaction energy $V_{E,\text{sphere}}^{(\text{CSCD})}$ (solid lines) and $V_{E,\text{sphere}}^{(\text{CPD})}$ (dashed lines) of the setup described in Fig. 3: (a) as a function of the angle θ between the electric field and the line connecting the sphere centers, for various center-to-center distances (indicated to the left, as multiples of the sphere diameter $l = 1$ μm), and (b) as a function of the center-to-center distance r, for various angles θ, indicated in the plot.

underestimates attractions at close distances, making it impractical for most applications. We conclude that, for spheres, the SSCD approach is therefore usually to be preferred over the other approaches.

C. Numerical results for cubes, cuboidal rods, spherocylinders, dumbbells, and misaligned particles

For brevity, we do not explicitly include the numerical results for cubes, cuboidal rods, spherocylinders, dumbbells, and misaligned particles in the body of this paper but instead refer the reader to the supplementary material[50] for additional details.

For cubes, neither the SSCD nor the SPD approach are very accurate: the former significantly overestimates attractions and also overestimates repulsions somewhat, and the latter underestimates attractions and significantly overestimates repulsions. The CPD approach gives results of comparably poor accuracy, but has as an added drawback its increased computational cost. Better results can be obtained by CSCD approaches where the number of chunks is reduced. Depending on the number of chunks chosen, these have relatively low computational cost and good accuracy.

For cuboidal rods with aspect ratio 1:5, reasonable results can only be obtained using techniques that employ multiple chunks per rod. Of the tested approaches, the CPD with 5 dipoles per rod is computationally cheapest but has as

drawback that it significantly overestimates repulsions. The accuracy of the CPD does not improve with increasing number of chunks per rod. Better accuracy can be obtained by using the CSCD approach with 5 chunks per rod.

For spherocylinders, the double charge approach discussed in IV A works very well, even outdoing some of the permanent dipole approaches. This could be of use in simulations, since it only uses four pair interactions per pair of spherocylinders.[52]

For dumbbells, the permanent dipole (CPD) approach and the double charge approach give results comparable in accuracy, with the double charge approach being better at estimating the maximum attraction and repulsion, and the CPD better at approximating the shape of the contour lines. As before, for increased accuracy the CSCD double dipole approach can be used. A significant disadvantage to the double charge method is, however, the fact that the Coulomb interaction is longer-ranged than the dipole-dipole interaction, which might complicate and slow down the simulations due to the more extensive Ewald summation it necessitates.

So far, we have only discussed particles that are perfectly aligned with the electric field and/or each other. For rods this is reasonable for strong enough electric fields, but might be problematic if the field is weaker. Cubes have been shown to not prefer any orientation in an electric field at all,[20] and hence a configuration of interacting nonaligned cubes is very reasonable to consider. Introducing the orientations of the particles into the problem, however, makes the parameter space extremely hard to systematically explore and, therefore, we restrict ourselves here to particles that are "as misaligned as possible." For rods, this means that one of the rod points along the field but the other lies perpendicular to it and for cubes, we consider a situation where, at $\theta = 0$, the corner of one cube points into the face of the other.

For misaligned rods of aspect ratio 1:5, similarly to aligned ones, the single-dipole approaches SSCD and SPD do not give good results and we therefore need to split up the particles into multiple chunks. Using the CPD will give fair results and is cheap if not many dipoles are used (which, as mentioned, has little influence on accuracy). However, the CPD has the problematic property that the location of maximum repulsion is situated in slightly the wrong place. If more accuracy is needed, the CSCD with 5 dipoles seems the best option. If long-range interactions are more important than short-range ones, it is advisable to include an extra correction factor to compensate for the fact that a $5 \times 1 \times 1$ cuboid has a different transverse polarizability than a $25 \times 5 \times 5$ one (the longitudinal polarizability being fixed), but this will negatively affect the accuracy at (very) short range.

For misaligned cubes, while all the approximations did relatively well, the self-consistent approaches clearly produced better results than their permanent-dipole counterparts. In particular, the SSCD did remarkably well, especially considering its relatively weak performance for aligned cubes. The CSCD approaches with low dipole numbers also did very well but we note that, because of the SSCD's excellent performance, the former seem necessary (for rotated cubes) only if a high level of precision is required.

V. CONCLUSION

We have introduced and generalized the Coupled Dipole Method (CDM) to include polarizable matter units that are not necessarily of atomic proportions. We used the CDM to derive an expression, identical to the one derived by Buckingham and Pople in 1955,[36] for the self-consistent interaction energy for two Lorentz atoms with isotropic polarizability and then proceeded to do the same for atoms with anisotropic polarizability. We compared these expressions to the commonly used method of pre-assigning dipole moments to calculate the interaction energy. We found that the expression derived for the latter method is a first-order Taylor approximation in r^{-3} of the "full" expression obtained using the self-consistent method.

We then proceeded to numerically evaluate the accuracy of various techniques for calculating the electric-field interaction energy of various particle shapes. The techniques considered were the "single permanent dipoles" (SPD) approach, where the particles are treated as point dipoles with pre-assigned dipole moments, the "single self-consistent dipoles" (SSCD) approach, where the particles are still treated as point dipoles but have self-consistent dipole moments, the "cluster of permanent dipoles" (CPD) approach, where the particles are split up into chunks with pre-assigned dipole moments, and the "cluster of self-consistent dipoles" (CSCD) approach, where the chunks instead have self-consistent dipole moments, calculated using the CDM. The particle shapes considered were spheres, cubes, rods, and dumbbells. For cubes and rods we considered the case where the particles are aligned with respect to each other and the electric field, and the case where the particles were "as misaligned as possible." For each shape and technique, the CSCD with the most dipole chunks was considered to be the "exact" result and the other techniques were judged according to their agreement with it.

We found that, for spheres, the SSCD approach does better than the other techniques, except the CSCD approach with a reduced number of dipoles. However, the latter is computationally expensive for the limited improvement it provides. The SPD and the CPD were found to give almost identical results, such that, if the permanent dipole approximation is used, there is no point in splitting up the sphere into multiple chunks.

For aligned cubes, neither the SSCD, SPD, nor CPD gave very satisfactory results. In this case, the SPD and CPD approaches do not give identical results, but the CPD approach is not more accurate than the SPD, such that, if using a permanent dipole approach, splitting up a cube into multiple chunks is not advisable. If using a self-consistent dipole approach, however, splitting up the cube into multiple chunks does improve the accuracy significantly, with a $3 \times 3 \times 3$ cube already giving decently accurate results (when compared to a $10 \times 10 \times 10$ cube). For misaligned cubes, the SSCD did better than the SPD and CPD (where, again, the latter is not more accurate than the former).

For rods, the CPD can be worthwhile. For cuboidal rods, splitting up the particle into multiple chunks is absolutely crucial for gaining accurate results, regardless of whether a

permanent or a self-consistent dipole approach is used. However, if using the CPD, the lowest possible number of chunks that gives the correct aspect ratio should be preferred, because splitting up the rod into more chunks does not significantly improve the accuracy of the CPD. With the CSCD, we saw good agreement even if using the lowest possible number of chunks. For spherocylindrical rods, we also examined a "double charge" (DC) approach, where a positive and a negative charge are placed at the ends of the rod. This approach produced slightly worse results when compared to a CPD approach with a high number of chunks, but slightly better results than CPD approaches with low numbers of chunks; its relative simplicity therefore makes it an interesting candidate for use in simulations.

For dumbbells, the DC approach was also tried. Here, it again achieved accuracy comparable to CPD approaches, but, in this case, the CPD approach only needs two dipoles per dumbbell. Since dipolar interactions are shorter-ranged than Coulomb interactions, the latter method might therefore be preferable computationally. A CSCD approach with only two Lorentz atoms per dumbbell produced better results than both the DC and CPD approach.

Speculating on the effects of using the interaction energy obtained from the SSCD approach instead of the result from the usual SPD for simulations, we note that the SSCD approach in general gives stronger attractions and weaker repulsions, especially at close distances. Therefore, it seems not unreasonable to assume that the SSCD would result in a widening of the parameter regime for which crystal phases such as body-centered tetragonal and body-centered orthorhombic lattices, which are based on shifted strings,[8–10,12] are stable. On the other hand, because repulsions are weaker, it becomes less important for a string to be shifted exactly half a unit cell with respect to its neighbors. As a consequence, we might also see more stable string fluids, where the particles form strings in the direction of the electric field, but where the strings are positionally disordered with respect to each other. Another interesting direction of research might be to study one of the interaction energies resulting from the CSCD or CPD.[53] The most obvious particle shape to investigate this for is the rod, since the effect of splitting up this particle into multiple chunks is significant even if the number of chunks is low, given the very bad agreement between the single dipole approaches (SSCD and SPD) and the CSCD result and the comparatively good accuracy of the cluster approaches (CPD and CSCD with a low number of chunks).

We note here that the SSCD and CSCD approaches, though they use self-consistent dipole moments, have, in this work, only been used to study interactions between particle pairs in the absence of other particles. It is of interest to investigate what effect the presence of other particles would have on these interactions; in other words, to study the many-body interactions between polarizable particles in an external electric field. This might be done in simulations, although the large-matrix manipulation involved in the CDM would make such simulations rather cumbersome with present-day computer power, but the many-body effects might also be investigated by, for example, simply studying the interaction between a pair of particles in the presence of a third particle. This is left for future study.

ACKNOWLEDGMENTS

This work is part of the research programme of FOM, which is financially supported by NWO. Financial support by an NWO-VICI grant is acknowledged.

[1] K. Bubke, H. Gnewuch, M. Hempstead, J. Hammer, and M. L. H. Green, Appl. Phys. Lett. **71**, 1906 (1997).
[2] A. F. Demirörs, P. M. Johnson, C. M. van Kats, A. van Blaaderen, and A. Imhof, Langmuir **26**, 14466 (2010).
[3] P. A. Smith, C. D. Nordquist, T. N. Jackson, T. S. Mayer, B. R. Martin, J. Mbindyo, and T. E. Mallouk, Appl. Phys. Lett. **77**, 1399 (2000).
[4] K. M. Ryan, A. Mastroianni, K. A. Stancil, H. Liu, and A. P. Alivisatos, Nano Lett. **6**, 1479 (2006).
[5] A. Yethiraj and A. van Blaaderen, Nature (London) **421**, 513 (2003).
[6] H. R. Vutukuri, J. Stiefelhagen, T. Vissers, A. Imhof, and A. van Blaaderen, Adv. Mater. **24**, 412 (2012).
[7] K. Kang and J. K. G. Dhont, Europhys. Lett. **84**, 14005 (2008).
[8] A.-P. Hynninen and M. Dijkstra, Phys. Rev. Lett. **94**, 138303 (2005).
[9] A.-P. Hynninen and M. Dijkstra, Phys. Rev. E **72**, 051402 (2005).
[10] F. Smallenburg and M. Dijkstra, J. Chem. Phys. **132**, 204508 (2010).
[11] F. Smallenburg, H. R. Vutukuri, A. Imhof, A. van Blaaderen, and M. Dijkstra, J. Phys.: Condens. Matter **24**, 464113 (2012).
[12] D. Levesque and J.-J. Weis, Mol. Phys. **109**, 2747 (2011).
[13] S. C. Glotzer and M. J. Solomon, Nat. Mater. **6**, 557 (2007).
[14] S.-M. Yang, S.-H. Kim, J.-M. Lima, and G.-R. Yi, J. Mater. Chem. **18**, 2177 (2008).
[15] J. D. Jackson, *Classical Electrodynamics*, 3rd ed. (John Wiley & Sons, Inc., 1999).
[16] P. I. C. Teixeira, M. A. Osipov, and M. M. Telo da Gama, Phys. Rev. E **57**, 1752 (1998).
[17] M. Renne and B. Nijboer, Chem. Phys. Lett. **1**, 317 (1967).
[18] B. Nijboer and M. Renne, Chem. Phys. Lett. **2**, 35 (1968).
[19] H.-Y. Kim, J. O. Sofo, D. Velegol, M. W. Cole, and G. Mukhopadhyay, Phys. Rev. A **72**, 053201 (2005).
[20] B. W. Kwaadgras, M. Verdult, M. Dijkstra, and R. van Roij, J. Chem. Phys. **135**, 134105 (2011).
[21] M. W. Cole and D. Velegol, Mol. Phys. **106**, 1587 (2008).
[22] H.-Y. Kim, J. O. Sofo, D. Velegol, M. W. Cole, and A. A. Lucas, J. Chem. Phys. **124**, 074504 (2006).
[23] S. M. Gatica, M. W. Cole, and D. Velegol, Nano Lett. **5**, 169 (2005).
[24] H.-Y. Kim, J. O. Sofo, D. Velegol, M. W. Cole, and A. A. Lucas, Langmuir **23**, 1735 (2007).
[25] E. M. Purcell and C. R. Pennypacker, Astrophys. J. **186**, 705 (1973).
[26] B. T. Draine, Astrophys. J. **333**, 848 (1988).
[27] C. F. Bohren and S. B. Singham, J. Geophys. Res. **96**, 5269, doi:10.1029/90JD01138 (1991).
[28] B. T. Draine and P. J. Flatau, J. Opt. Soc. Am. A **11**, 1491 (1994).
[29] B. W. Kwaadgras, M. Dijkstra, and R. van Roij, J. Chem. Phys. **136**, 131102 (2012).
[30] A. Sihvola, J. Nanomater. **2007**, 45090 (2007).
[31] A. Sihvola, P. Yla-Oijala, S. Jarvenpaa, and J. Avelin, IEEE Trans. Antennas Propag. **52**, 2226 (2004).
[32] H. Kettunen, H. Wallen, and A. Sihvola, J. Appl. Phys. **102**, 044105 (2007).
[33] M. Pitkonen, J. Appl. Phys. **103**, 104910 (2008).
[34] M. Pitkonen, J. Math. Phys. **47**, 102901 (2006).
[35] M. Mandel and P. Mazur, Physica **24**, 116 (1958).
[36] A. D. Buckingham and J. A. Pople, Trans. Faraday Soc. **51**, 1029 (1955).
[37] A. D. Buckingham, J. Chem. Phys. **23**, 2370 (1955).
[38] A. D. Buckingham and J. A. Pople, J. Chem. Phys. **27**, 820 (1957).
[39] A. Isihara, Physica **27**, 857 (1961).
[40] J. Ramshaw, Physica **62**, 1 (1972).
[41] E. F. O'Brien, V. P. Gutschick, V. McKoy, and J. P. McTague, Phys. Rev. A **8**, 690 (1973).

[42]L. Galatry and T. Gharbi, Chem. Phys. Lett. **75**, 427 (1980).
[43]B. Cichocki and B. Felderhof, J. Stat. Phys. **53**, 499 (1988).
[44]C. Jarque and A. D. Buckingham, J. Chem. Soc., Faraday Trans. **88**, 1353 (1992).
[45]A. D. Buckingham and Y. Tantirungrotechai, Can. J. Chem. **77**, 1946 (1999).
[46]A. J. Stone, Y. Tantirungrotechai, and A. D. Buckingham, Phys. Chem. Chem. Phys. **2**, 429 (2000).
[47]A. Baranowska, B. Fernandez, A. Rizzo, and B. Jansik, Phys. Chem. Chem. Phys. **11**, 9871 (2009).
[48]B. W. Kwaadgras, M. W. J. Verdult, M. Dijkstra, and R. van Roij, J. Chem. Phys. **138**, 104308 (2013).
[49]C. Kittel, *Introduction to Solid State Physics*, 7th ed. (John Wiley & Sons, Inc., 1996).
[50]See supplementary material at http://dx.doi.org/10.1063/1.4870251 for additional information.
[51]W. H. Press, S. A. Teukolsky, W. T. Vetterling, and B. P. Flannery, *Numerical Recipes: The Art of Scientific Computing*, 3rd ed. (Cambridge University Press, 2007).
[52]T. Troppenz, L. Filion, R. van Roij, and M. Dijkstra, "Phase behavior of polarizable colloidal hard rods in an external electric field: a simulation study" (unpublished).
[53]F. Smallenburg, "Clustering and self-assembly in colloidal systems," Ph.D. thesis, Utrecht University, 2012.